coatings

MDPI

Article

Effect of Nano-TiO_2 on Capillary Water Absorption of Recycled Aggregate Concrete

Chuheng Zhong [1], Zhiling Yu [1], Jinzhi Zhou [1,2,*], Yuhua Long [1], Peng Tian [1] and Jinhui Chen [3,4]

[1] School of Civil Engineering, Architecture and Environment, Hubei University of Technology, Wuhan 430068, China
[2] State Key Laboratory for Health and Safety of Bridge Structures, Wuhan 430034, China
[3] School of Public Policy and Management, Tsinghua University, Beijing 100084, China
[4] High-Tech Research and Development Center, Ministry of Science and Technology, Beijing 100044, China
* Correspondence: zhoujinzhi@hbut.edu.cn

Abstract: To improve the durability performance of recycled aggregate concrete in actual use, this paper uses nano-TiO_2-modified recycled coarse aggregate to study, through experiments, the effects of nano-TiO_2 on the pore distribution of recycled coarse aggregate concrete after freeze–thaw. The capillary-water-absorption law was used as the evaluation index. The recycled coarse aggregate concrete was prepared with different contents of nano-TiO_2, and changes in the 24 h capillary water absorption and porosity of the recycled aggregate concrete after freeze–thaw cycles were analysed. With the help of high-resolution image recognition and binary-image-processing technology, the pore distribution of the recycled aggregate concrete before and after freeze–thaw cycles was obtained. Through the analysis of the water-absorption data at different times, the initial capillary-water-absorption rate, S_1, is obtained. The capillary water absorption of recycled aggregate concrete is reacted with S_1, and the initial capillary-water-absorption prediction model of nano-TiO_2 recycled aggregate concrete under freeze–thaw cycles is established. The results show that under the action of freeze–thaw cycles, the capillary water absorption of recycled coarse aggregate concrete increases with the increase in the RCA substitution rate and decreases with the increase in nano-TiO_2 content. After 150 freeze–thaw cycles, the cumulative water absorption and porosity of RC25-NT1.2 decreased by 25.52% and 14.57%, respectively, compared with the test block without nanomaterials. It was found that nano-TiO_2 has a prominent role in modifying recycled aggregate concrete. Nano-TiO_2 can reduce the cumulative water absorption and porosity of recycled aggregate concrete and alleviate the negative impact of the recycled coarse aggregate on capillary water absorption of concrete after freeze–thaw cycles. It was observed by scanning electron microscopy that a large amount of C–S–H gel was produced inside the concrete mixed with nano-TiO_2, which bonded the internal pores and cracks to form a dense structure.

Keywords: nano-TiO_2; recycled aggregate concrete; freeze–thaw cycle; capillary water absorption; porosity

Citation: Zhong, C.; Yu, Z.; Zhou, J.; Long, Y.; Tian, P.; Chen, J. Effect of Nano-TiO_2 on Capillary Water Absorption of Recycled Aggregate Concrete. *Coatings* **2022**, *12*, 1833. https://doi.org/10.3390/coatings12121833

Academic Editor: Paolo Castaldo

Received: 4 November 2022
Accepted: 22 November 2022
Published: 26 November 2022

1. Introduction

Due to the expansion of urban reconstruction and transportation routes, a large amount of waste concrete has been produced, which has also led to the increasing use of concrete and the shortage of natural resources. Usually, waste concrete will be treated as garbage backfill, which takes up a lot of land resources and has a certain degree of impact on the ecological environment [1,2]. To meet the development requirements of green sustainability, the waste concrete produced by demolishing buildings is recycled, crushed, graded, cleaned, and mixed in a certain proportion and gradation to form recycled concrete aggregate (RCA). Comprehensive utilization of construction solid waste to achieve construction waste diversion [3,4]. Due to the presence of a layer of hardened cement mortar on the surface of RCA, discontinuous porous areas appear between the old

aggregate and the cement paste, resulting in a low aggregate-crushing index, high water absorption, and low apparent density [5,6]. When RCA is directly used in concrete, harmful substances can easily erode the concrete through ion diffusion, capillary adsorption, and pressure penetration [7,8], thus weakening the bearing capacity of building structures and threatening the safety and durability of buildings [9,10].

In high latitudes, water intrusion will accelerate the deterioration of concrete freeze–thaw cycles. When the concrete is saturated, the water transport in the pores is mainly caused by the internal pressure gradient and gravity, but this rarely occurs. When the concrete is unsaturated, the harmful substances in the internal pores are mainly invaded by capillary adsorption, so the capillary pores are the most easily invaded and damaged area by water during the freeze–thaw cycle [11,12]. The modification of RCA can effectively delay water intrusion, enhance the ability of concrete to resist freeze–thaw cycles, reduce the capillary adsorption capacity of concrete, and improve its durability [13,14]. El-Hawary et al. [15] studied the resistance of recycled aggregate concrete to freeze–thaw cycles under different replacement rates and found that the use of slag with high-pozzolanic activity instead of cement can enhance the durability of concrete containing 50% RCA. Santana et al. [16] subjected recycled aggregate concrete of different strength classes (C30 and C60) to freeze–thaw cycles and found that the density values of RAC were lower than those of natural concrete of both strength classes. All concrete mixtures of C35 and C60 grades showed a reduction in compressive and tensile strength as well as concrete quality after 150 and 300 freeze–thaw cycles. RCA increases the porosity of concrete and reduces the compressive strength, tensile strength, and durability of concrete. Through low-field nuclear magnetic resonance technology and scanning electron microscopy, Wang et al. [17] found that an air-entraining agent can cut off the connectivity of capillary pores inside the mortar so that the internal cracks of concrete after freeze–thaw cycles are not interconnected, which can delay water diffusion and reduce the capillary-water-absorption coefficient of concrete. Deboucha et al. [18] used blast-furnace slag and volcanic ash to fill the internal structure of concrete and found that the zeolite reaction produced by blast-furnace slag can promote the formation of C–S–H gel, improve the size and distribution of capillary pores, and 30% of blast-furnace slag improves the strength grade of concrete.

In recent years, nanomaterials have attracted much attention for improving the durability of concrete due to their large specific surface area, high surface activity, and strong oxidizing properties [19,20]. Nano-TiO_2 has photocatalytic properties, as well as antibacterial and self-cleaning properties [21,22]. These characteristics can use sunlight to mineralize organic pollutants into CO_2 and H_2O. As a new type of building material, nano-TiO_2 can improve the internal structure of concrete, degrade pollutants, and achieve green environmental protection. Liu et al. [23] studied the internal deterioration of concrete mixed with nano-SiO_2 and nano-TiO_2 with different particle sizes under freeze–thaw cycles by employing nuclear magnetic resonance and CT scanning. The study confirmed that the smaller the particle size of the nanomaterials, the denser the internal structure of the concrete. Under the same particle size, the experimental effect of nano-TiO_2 is better than that of nano-SiO_2. Ying et al. [24] added nano-SiO_2 and nano-TiO_2 to recycled aggregate concrete and tested the porosity by the pressure-pump method. The results show that nanoparticles play a unique role in refining the pore structure of recycled aggregate concrete, enhancing the diffusion resistance of recycled aggregate concrete to chloride, and effectively improving the durability of recycled aggregate concrete. Chen et al. [25] compared the effects of two types of nano-TiO_2 on the hydration and properties of cement and found that nano-TiO_2 had the effect of catalysing the hydration of cement. Inertia and stability reduced the total porosity of cement slurry and the pore size was refined, which had a significant effect on the physical properties and mechanical energy of cementitious materials.

The above research shows that the pore distribution of concrete is an important part to study the frost resistance of concrete. Nanomaterials can affect the internal structure and porosity of concrete, but there are relatively few studies on the combination of freeze–thaw cycles and pore development. In this paper, nano-TiO_2-modified RCA was used to study

the 24 h capillary-water-absorption performance of recycled aggregate concrete before and after freeze–thaw cycles. The surface-pore-distribution characteristics and internal-influence mechanism were analysed and studied using Matlab software and SEM scanning electron microscopy. The initial capillary-water-absorption prediction model of nano-TiO_2 recycled aggregate concrete under freeze–thaw cycles was established.

2. Materials and Methods

2.1. Materials and Specimen Making

The cement used was Huaxin P·O 42.5 ordinary portland cement. The natural coarse aggregate adopts graded common gravel with a particle size of 5–25 mm. The waste concrete with strength grades C40 and C50 was crushed by a jaw crusher to obtain the RCA. After cleaning and drying to remove impurities, aggregates with a particle size of 5–25 mm were manually sieved, which were used to replace the natural coarse aggregate by a ratio of 25%, 50%, and 75%. Nano-TiO_2 replaced the cement with a ratio of 0.4%, 0.8%, and 1.2%, respectively. The fine aggregate was the natural river sand, with a mud content of less than 1%. The admixture is a polycarboxylate superplasticizer, and the water reduction rate was 20%. All materials were mixed with tap water. Silicate cement parameters are shown in Table 1; NA parameters are shown in Table 2; RCA parameters are shown in Table 3; Nano-TiO_2 parameters are shown in Table 4; and polycarboxylate superplasticizer parameters are shown in Table 5. The mix proportion of nano-TiO_2 recycled concrete is shown in Table 6.

Table 1. Cement main technical parameters.

Density(g/cm^3)	Setting Time(h)		Compressive Strength (MPa)	Standard Consistency Water (%)	Specific Surface Area (m^2/kg)
	Initial	Termination			
0.3%	1.9	2.35	49.8	30	Low heat

Table 2. NA physical indicators.

Grain Size (mm)	Apparent Density (kg/m^3)	Stacking Density (kg/m^3)	Water-Absorption Rate (%)	Crushing Index (%)
5~25	2300	1600	0.45	6.8

Table 3. RCA physical indicators.

Grain Size (mm)	Apparent Density (kg/m^3)	Stacking Density (kg/m^3)	Water-Absorption Rate (%)	Crushing Index (%)
5~25	2390	1304	6.3	15.7

Table 4. Nano-TiO_2 main technical parameters.

Particle Size (nm)	Purity (%)	Specific Surface Area (m^2/g)	Density (g/cm^3)	Crystal Form
25	99.9	160	3.9	Anatase

Table 5. Polycarboxylate superplasticizer main technical parameter.

Specification Model	Water Reduction Rate (%)	Gas Content (%)	Water Content (%)	Total Alkali Amount (%)	PH Value
FK-A	≥20	≤6.0	≤3.0	≤10.0	7.0 ± 1.0

Table 6. Mix ratio of nano-TiO_2 recycle aggregate concrete (kg/m^3).

Test-Block Number	Material Dosage (kg/m^3)						
	Cement	Sand	Water	NA	RCA	NT	Water Reducer
RC25	450	669	180	818.75	272.25	0	3.6
RC25-NT0.4	448.2	669	180	818.75	272.25	1.8	2.25
RC25-NT0.8	446.4	669	180	818.75	272.25	3.6	3.6
RC25-NT1.2	444.6	669	180	818.75	272.25	5.4	5.4
RC50	450	669	180	545.5	545.5	0	4.05
RC50-NT0.4	448.2	669	180	545.5	545.5	1.8	2.25
RC50-NT0.8	446.4	669	180	545.5	545.5	3.6	3.6
RC50-NT1.2	444.6	669	180	545.5	545.5	5.4	5.4
RC75	450	669	180	272.75	818.25	0	4.5
RC75-NT0.4	448.2	669	180	272.75	818.25	1.8	2.25
RC75-NT0.8	446.4	669	180	272.75	818.25	3.6	3.6
RC75-NT1.2	444.6	669	180	272.75	818.25	5.4	5.4

NC is the natural coarse aggregate; NT is nano-TiO_2.

2.2. Test Method

2.2.1. Capillary-Water-Absorption Test after Freeze–thaw Cycles

Freeze–thaw cycling tests were performed according to the quick-freeze method in 'Standard for test methods of long-term performance and durability of ordinary concrete' [26]. Three test blocks of 100 mm × 100 mm × 400 mm were made for each group. After 24 days of maintenance under standard curing conditions, the test block was taken out and immersed in constant-temperature water at (20 ± 2) °C for 4 days. When the recycled aggregate concrete reached 50, 100, and 150 freeze–thaw cycles, it was taken out for the capillary-water-absorption test. Figure 1 shows the test-block preparation and maintenance, and Figure 2 shows the rapid freeze–thaw cycle test.

Figure 1. Test-block preparation and maintenance.

In the capillary-water-absorption test, a small cuboid sample with the size of 100 mm × 100 mm × 50 mm was cut from the freeze–thawed sample along the central area, and then dried in an oven at (85 ± 5) °C for 48 h. First, the test block's four vertical pouring surfaces were evenly coated with an epoxy resin adhesive seal, and the top was covered with plastic film to ensure that only the lower facade of the test block would be in contact with water. Then, the original quality of the test block was weighed after the epoxy

resin solidified. Finally, the sealed test block was put into the water-absorption device in turn, and the liquid level was kept 1~ 3 mm higher than the bottom of the test block. At the corresponding water-absorption time, the test block was quickly removed, and excess water was quickly wiped off at the bottom of the test block with a wet wipe. The mass difference before and after water absorption of the sample was calculated by weighing. The test process is shown in Figure 3, and the capillary-water-absorption interval time is shown in Table 7.

Figure 2. Fast freeze–thawing test.

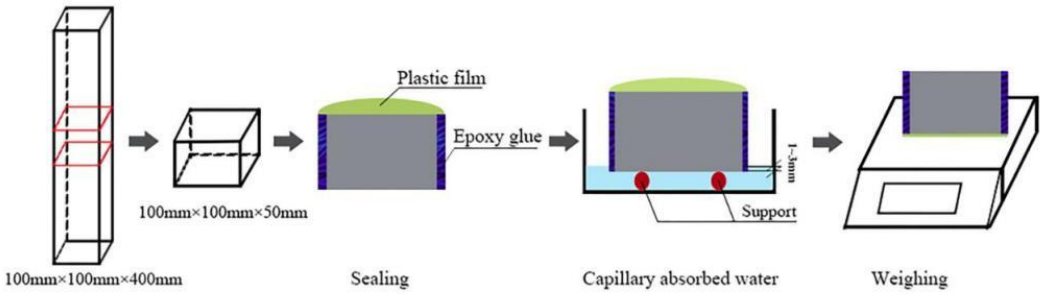

Figure 3. Capillary-water-absorption test flow chart.

Table 7. Test time intervals and allowable errors.

Test Interval	Permissible Error	Test Interval	Permissible Error
5 min	0 s	4 h	2 min
10 min	0 s	5 h	2 min
20 min	1 min	6 h	2 min
30 min	2 min	18 h	1 h
60 min	2 min	20 h	2 min
2 h	2 min	22 h	2 min
3 h	2 min	24 h	2 min

2.2.2. Pore Test

The water-absorption section of the test block was filled with white building gypsum and naturally dried in a cool environment. After the gypsum surface was completely hardened, the filling surface was polished by a grinding and polishing machine to a smooth surface without excess gypsum. A high-power pixel camera was used to image the polished specimen section in the same environment. Figure 4 is the flow chart of the binary-processing test-block pore. Figure 4a shows the recycled aggregate concrete test block without any treatment. There is a small amount of cement mortar peeling around the test block. The corners are smooth, and there are many scattered and irregular hemispherical pores and some discontinuous microcracks formed by small pores on the suction surface. Figure 4b is a polished and smooth effect drawing of the water-absorption surface after being filled with white building gypsum, which reflects the orientation and size of the water-absorption face pore. Figure 4c is a binary image, the black parts are the gypsum-filled pores, and the white part is recycled aggregate concrete (including all aggregates and

cement mortar). Finally, the internal fragments of RCA samples were taken and scanned by electron microscope after gold-spraying to analyse the microstructure characteristics of nano-TiO_2 recycled aggregate concrete before and after freeze–thaw cycles under different shooting specifications. To describe the pores of the water-absorbing surface of the recycled concrete more directly, the images were identified by using Matlab software as grayscale maps, and the porosity of the water-absorbing surface of the nano-TiO2 recycled concrete was calculated. To reduce the error caused by the peeling of the skin of the test block due to the freeze–thaw-cycle test, when calculating the porosity, the surface area V of the absorbing water surface is uniformly taken as 90 mm × 90 mm, as shown in Formula (1).

$$p = \frac{V_k}{V} \tag{1}$$

where p is porosity (%); V_k is the pore area (mm^2); and V is the suction surface area of the test block (mm^2).

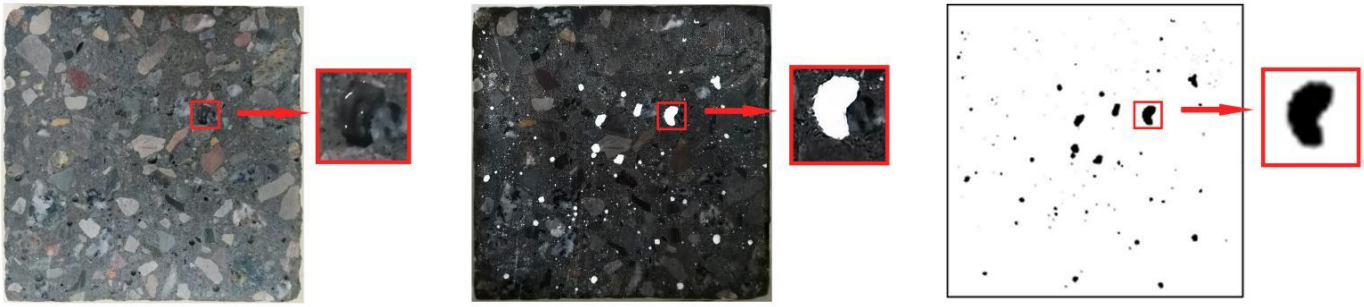

(**a**) (**b**) (**c**)

Figure 4. Pore flow chart of binarization processing test block. (**a**) Untreated test blocks; (**b**) test block after grinding; (**c**) completed test blocks.

3. Results and Discussion

3.1. Capillary-Water-Absorption Test

3.1.1. Cumulative Water Absorption

In general, the cumulative water absorption per unit area I is used to describe the ability of water to transfer inside the recycled aggregate concrete under freeze–thaw cycles, as shown in Formula (2).

$$I = \frac{M_t}{A\rho} \tag{2}$$

where I is the cumulative water absorption per unit area (mm); M_t is the mass difference of the test block before and after water absorption (g); A is the contact area between the test block and water (mm); and ρ is the density of water (g/mm^3).

By measuring the mass difference before and after the water absorption of the test block in unit time, the relationship between the cumulative water absorption per unit area of nano-TiO_2 recycled aggregate concrete and the square root of time under different freeze–thaw cycles, R25, R50, and R75 (three groups of different RCA content), as shown in Figure 5. The cumulative water absorption per unit area of the test block increases sharply in the first 6 h ($t^{1/2}$ = 147 s) and then tends to level off. The variation in the accumulated water absorption I of the test block can be roughly divided into two stages: primary absorption and secondary absorption.

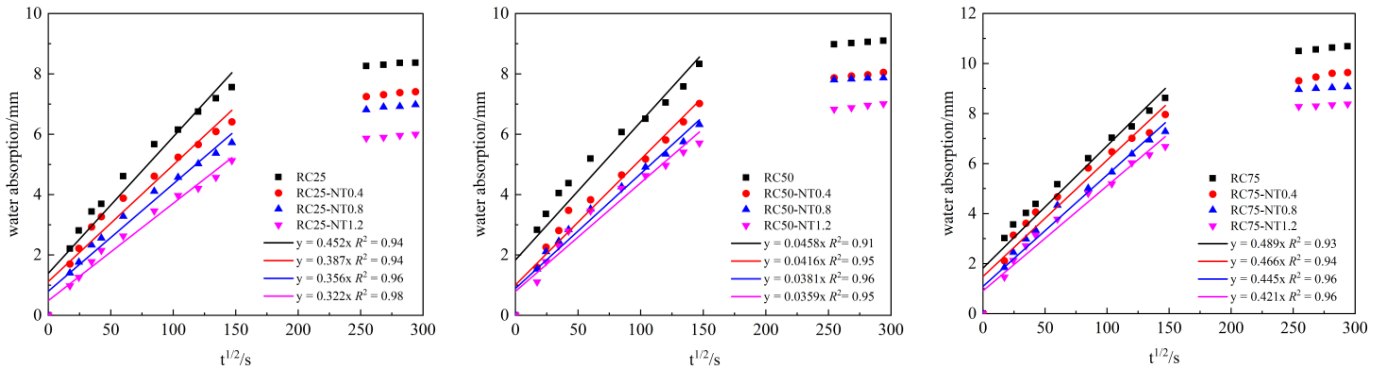

(**a**)

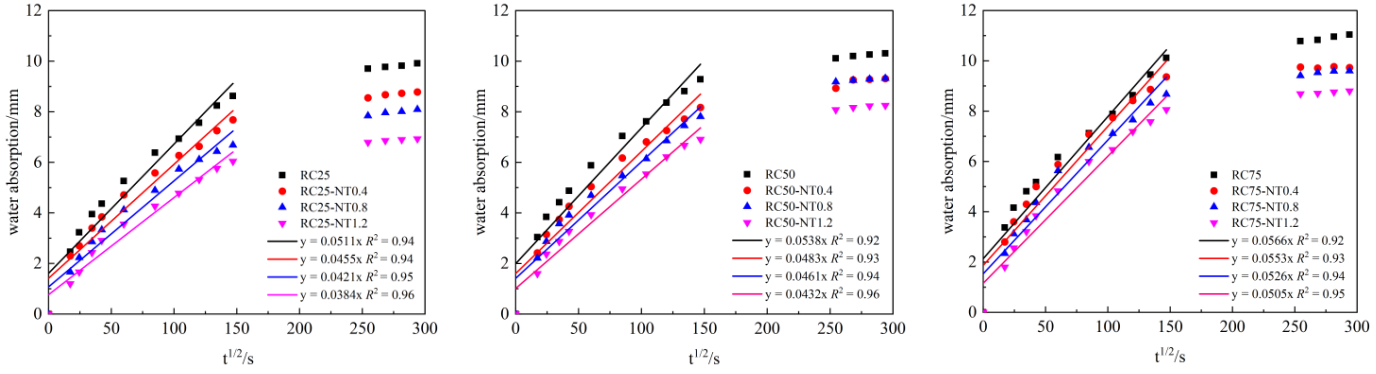

(**b**)

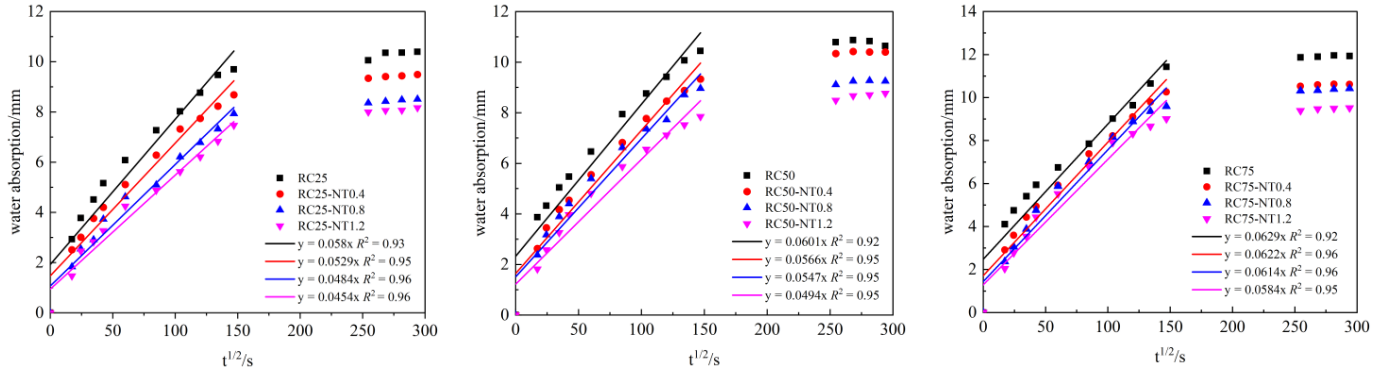

(**c**)

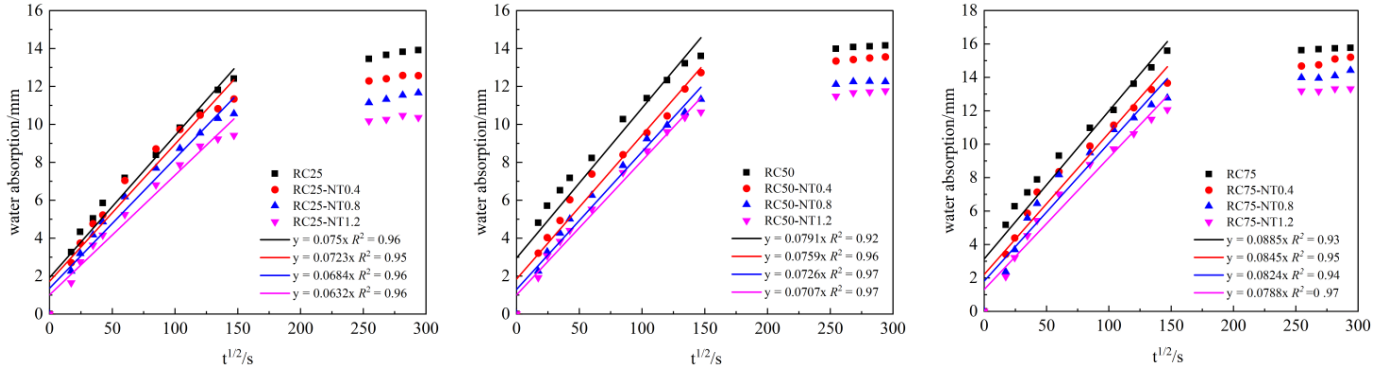

(**d**)

Figure 5. Cumulative water absorption and time–square-root relationship diagram. (**a**) n = 0; (**b**) n = 50; (**c**) n = 100; (**d**) n = 150.

When the RCA doping is the same, the cumulative water absorption of the four test-block groups varies as follows: NT0 < NT0.4 < NT0.8 < NT1.2. It can be seen from the figure that the cumulative water absorption of the three test-block groups was not much different in the first 60 min. With the increase in time and the number of freeze–thaw cycles, the cumulative water absorption of the test blocks without nano-TiO_2 continued to rise. In the whole process of freeze–thaw cycles, the cumulative water absorption of the R25 group was relatively stable. In the R50 group, the overall upward trend of RC50 was large, and the upward trend of NT0.4 and NT0.8 was close when freeze–thawed 50 times and 100 times, and the changing trend of water absorption was not large. The R75 group showed a more obvious upward trend, with the highest water absorption. During the whole water-absorption process, the effect of nano-TiO_2 content on the R75 group was not as obvious as that of the previous two groups, and the cumulative water absorption of the three test-block groups was the best when the nano-TiO_2 content was 1.2 %. Specifically, when the freeze–thaw cycle was zero times, the cumulative water absorption of the three groups of nano-TiO_2 test blocks with 1.2% content was reduced by 28.3%, 22.97%, and 21.61%, respectively, compared with the undoped. At 150 times of freezing and thawing, the reduction was 25.52%, 16.88%, and 15.48%, respectively. It can be seen that the larger the amount of nano-TiO_2 added, the higher the cumulative-water-absorption decline rate.

When the RCA content was different, the cumulative water-absorption trend of the test block was R25 group < R50 group < R75 group. With the increase in RCA content, the cumulative-water-absorption trend of the test block decreased. Compared with RC50 and RC75, the cumulative water absorption of RC25 decreased by 8.02% and 21.7%, respectively, at 0 freeze–thaw cycles, and decreased by 3.86% and 11.74%, respectively, at 150 freeze–thaw cycles.

3.1.2. Water Absorption

Using water absorption S instead of the capillary coefficient is an important index to describe the water-absorption performance of recycled aggregate concrete, which is widely used to evaluate the water-absorption characteristics of building materials. After fitting the two stages of cumulative water absorption I, the initial water absorption S_1 ($t^{1/2}$ = 0–147 s) and the secondary water absorption S_2 ($t^{1/2}$ = 147–294 s) of recycled aggregate concrete can be obtained, as shown in Formula (3):

$$I = S\sqrt{t} \tag{3}$$

where S is water absorption ($mm/s^{1/2}$) and t is time (s).

Figure 6 shows the relationship between the initial capillary-water-absorption rate S_1 and the number of freeze–thaw cycles n. According to the diagram, the initial capillary-water-absorption rate S_1 of the three groups of recycled aggregate concrete shows an upward trend, the growth rate is faster with time, and the water absorption is more.

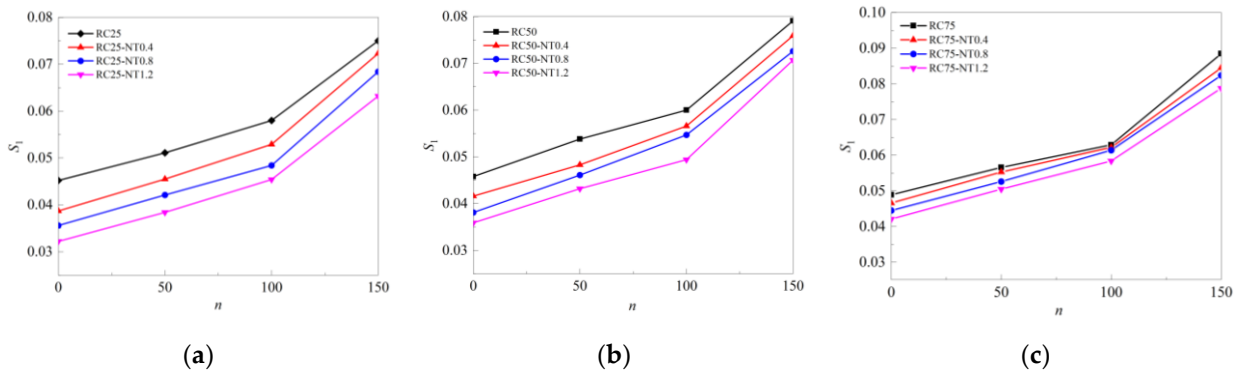

Figure 6. The variation curve of initial water absorption S_1 with freezing–thawing cycle n. (**a**) R25 group; (**b**) R50 group; (**c**) R75 group.

Under the condition of no nanomaterials, the maximum differences in S_1 of RC25, RC50, and RC75 reached 39.73%, 42.1%, and 44.75%, respectively, when the freeze–thaw cycle was 0 and 150 times. It can be seen that the freeze–thaw cycle has a direct impact on the water absorption of recycled aggregate concrete. This is because when RCA is recycled, a large amount of residual original cement mortar will form an interface transition zone (ITZ) with high porosity and a large number of microcracks on the aggregate surface. ITZs can easily weaken the bearing capacity and stability of concrete. When the test block is in a freeze–thaw environment, the seepage pressure and hydrostatic pressure make the water in the ITZ continue to move [27,28]. When the pressure reaches a certain level, the fine cracks contained in the RCA are expanded, increased, and connected, resulting in the generation of new cracks driven by the original cracks. Under the action of capillary force, the water invades rapidly, and S_1 rises sharply. Therefore, the S_1 of R75 is higher than that of the other two groups.

After adding nanomaterials, the water absorption of recycled aggregate concrete decreased significantly. Before freezing and thawing, the water-absorption rate of the three groups of specimens with 1.2% nano-TiO_2 content was reduced by 28.76%, 21.62%, and 13.9%, respectively, compared with those without nanomaterials. When the freeze–thaw cycle was 150 times, it was reduced by 15.73%, 10.62%, and 10.96%, respectively. It can be seen that the incorporation of nano-TiO_2 can reduce the water absorption of recycled aggregate concrete to varying degrees, and the less the RCA content, the better the effect. Because nano-TiO_2 is a "zero-dimensional structure" nanoparticle with a size much smaller than cement particles, it can accelerate $CA(OH)_2$ formation as a nucleation site of $CA(OH)_2$ crystals, promote cement hydration, affect the microporous structure of cementitious composites, and can fill and repair the pores and cracks of recycled concrete ITZs (to some extent), and improve their physical properties [29,30]. Secondly, nano-TiO_2 is a kind of nonreactive fine filler without doping activity. It has stability and inertia, which can accelerate the hydration rate of cement, increase the reaction area between RCA and cement paste, and produce more C–S–H gel [31]. The photocatalytic effect makes nano-TiO_2 have strong cohesiveness in cement-based composites. With the increase in dosage, the filling effect of the cement mixture is more sufficient, the channel of water entering the concrete is reduced, and the compactness of the recycled aggregate concrete is improved.

Macroscopically, the density of the S_1 curve of the three groups of recycled aggregate concrete is R75 > R50 > R25. This is because the higher the RCA content, the lower the internal compactness of the concrete, and the same amount of nano-TiO_2 cannot be filled. If the content of nano-TiO_2 is too high, the material will gather due to the agglomeration effect, reduce the average spacing between particles, and limit the formation of $Ca(OH)_2$ [32]. Overall, among the three groups of different nano-TiO_2 recycled aggregate concrete, the combination of 25% RCA and 1.2% nano-TiO_2 is the best.

Figure 7 is the relationship between the secondary capillary-water-absorption rate S_2 and the number of freeze–thaw cycles n of nano-TiO_2 recycled aggregate concrete with different dosages. Different from S_1, with the increase in freeze–thaw cycles, the growth rate of S_2 slowed down, the water absorption changed little, and the numerical change trend between groups was very small. This is because the recycled aggregate concrete in the early capillary-water-absorption rate is relatively fast; with the extension of time, the natural water absorption of the test block gradually reached a saturated state, resulting in the test block's later water-absorption rate being relatively slow, and the water absorption being greatly reduced.

It can be analysed from the change curves of S_1 and S_2 that the water-absorption index can fully reflect the water-absorption performance of recycled aggregate concrete. The incorporation of nano-TiO_2 can reduce the water-absorption performance of recycled aggregate concrete and effectively improve the freeze–thaw resistance. Therefore, the use of recycled aggregate concrete in severe cold regions can fully consider the superiority of nano-TiO_2.

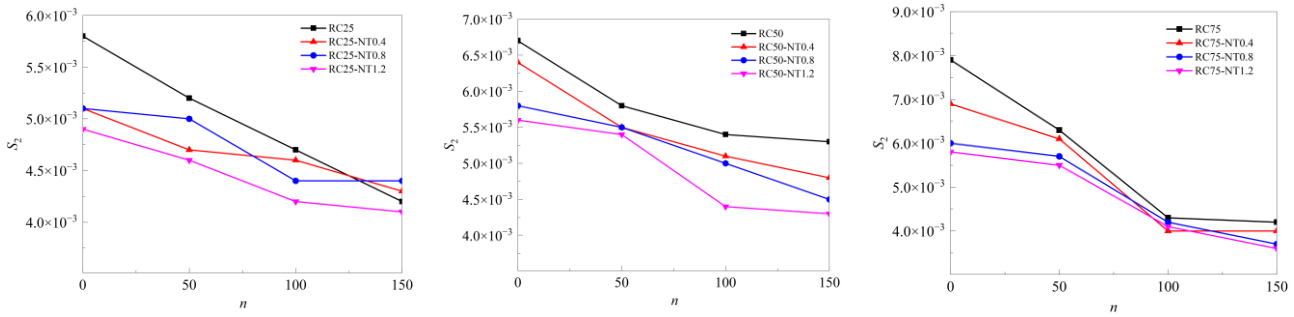

Figure 7. The variation curve of initial water absorption S_2 with freezing–thawing cycle n. (**a**) R25 group; (**b**) R50 group; (**c**) R75 group.

3.2. Pore Analysis

In the abovementioned cumulative water-absorption test, the testing effect of a nano-TiO_2 content of 1.2% is the best. Therefore, the nano-TiO_2 recycled aggregate concrete with this content is taken for pore analysis at the water-absorption surface at 0 and 150 freeze–thaw cycles. Figures 8 and 9 are the pore-structure distribution maps of the two groups after treatment. Table 8 is the macroscopic porosity and maximum pore size of the recycled aggregate concrete suction surface.

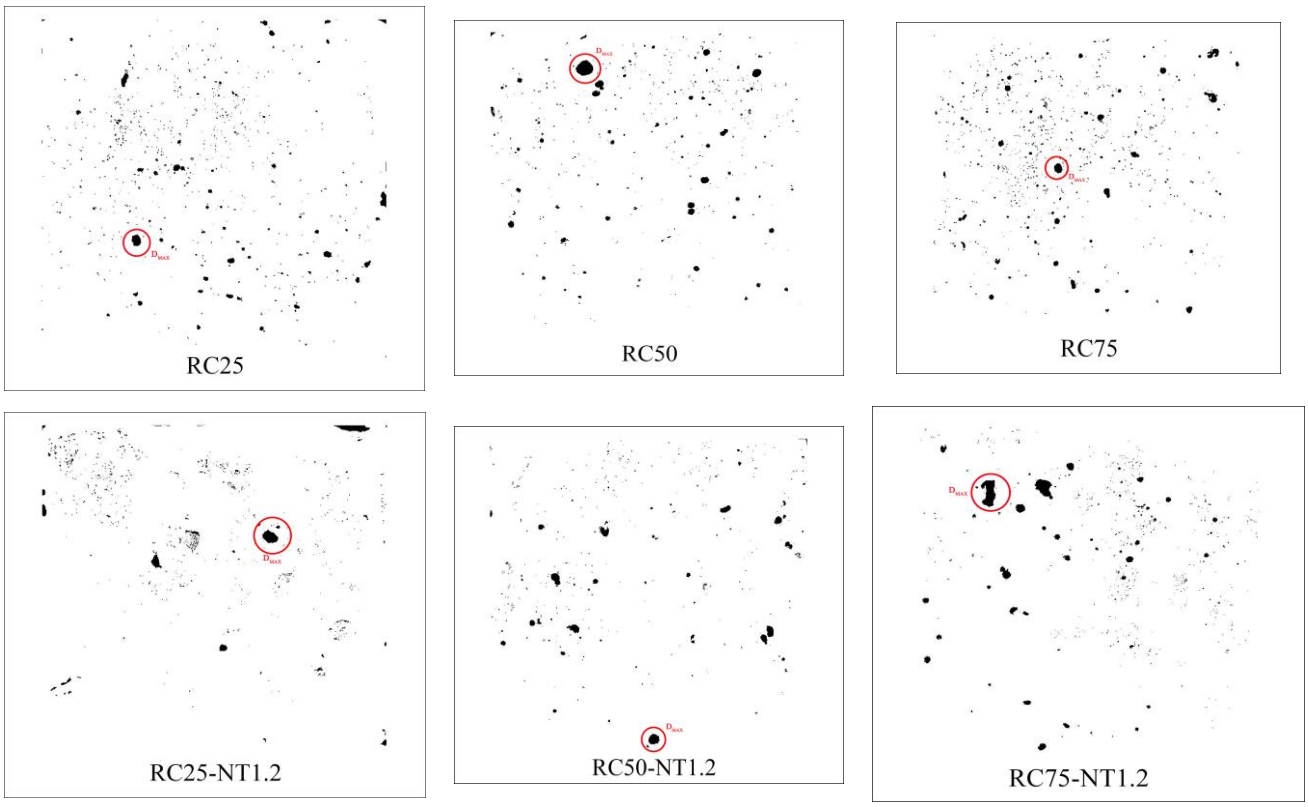

Figure 8. Macroscopic pore diagram of recycled aggregate concrete without freeze–thaw.

Without freeze–thaw cycle, the test-block had a suction surface distribution of a large number of closed pores. After 150 freeze–thaw cycles, the large pores in the test block were affected by freeze–thaw damage, and the pore size increased significantly, especially RC75. Part of the pores was connected and developed into intermittent cracks, which continuously deepened the damage of the freeze–thaw cycles. After adding 1.2% nano-TiO_2, the pores on the surface of the test block without freeze–thaw were gradually refined,

the large pores were prominent, and the overall number of pores was significantly reduced. After 150 freeze–thaw cycles, some small pores in RC25 were filled, and some small pores developed into large pores. RC50 small pores gradually developed into cracks; compared to the other two groups, the number of large pores was less. For RC75, although the overall porosity decreased, some pores became larger after freeze–thaw cycles, and the freeze–thaw damage was serious. In Table 8, the maximum pore size of the absorption surface becomes larger with increasing freeze–thaw cycles. When not freeze–thawed, the porosity of the water-absorption surface of the three groups of specimens doped with 1.2% nano-TiO_2 decreased by 21.13%, 21.97%, and 12.86%, respectively, compared with the undoped ones, and decreased by 14.57%, 15.33%, and 6.47% after 150 cycles of freeze–thawing. This indicates that the RCA admixture directly affects the porosity of recycled concrete, while nano-TiO_2 can fill part of the pores of recycled concrete and reduce the porosity. However, under the dual action of RCA and freeze–thaw cycles, part of the pores not filled by nano-TiO_2 continue to produce damage, so freeze–thaw cycles are a key factor in destroying the internal structure and compactness of recycled concrete.

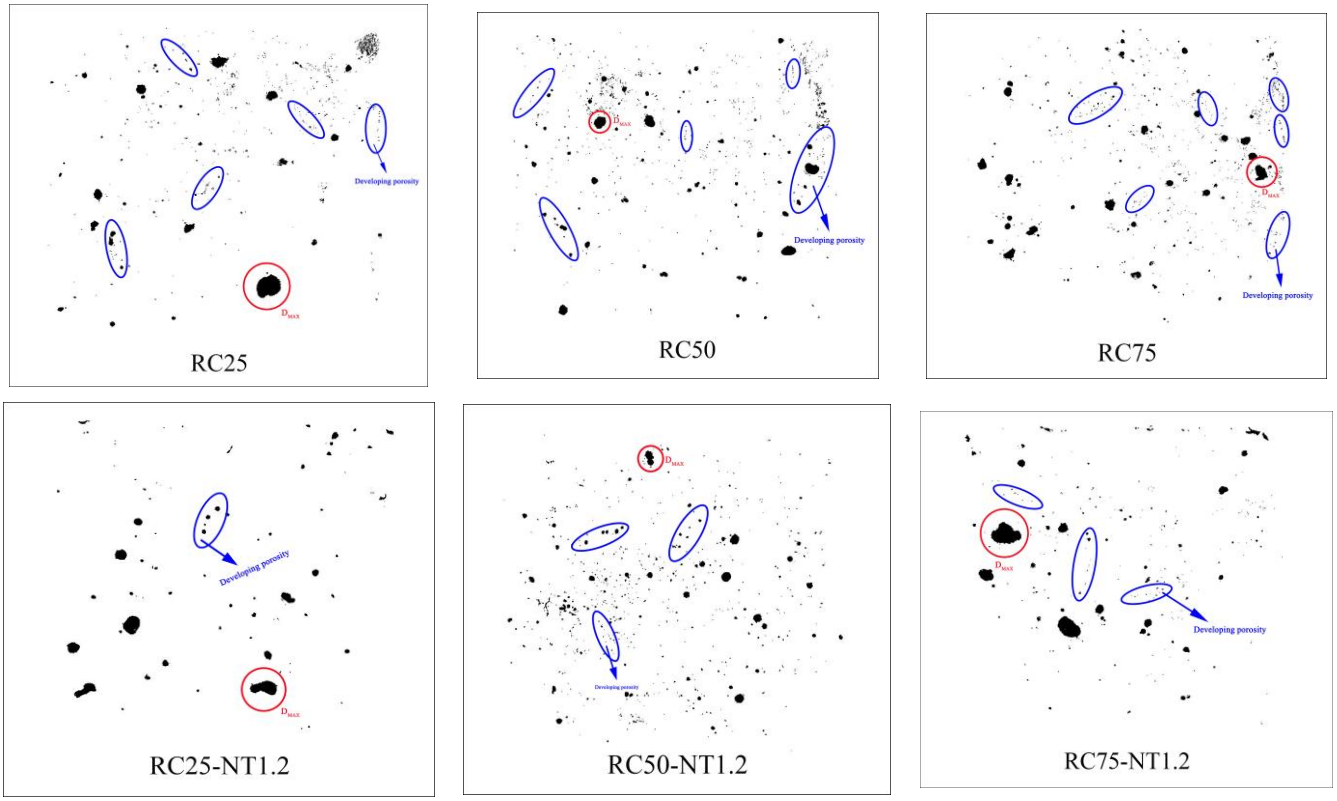

Figure 9. Macroscopic pore diagram of recycled aggregate concrete at 150 freeze–thaw cycles.

Table 8. Macroscopic porosity (%) and maximum pore diameter (mm).

Number	Not Freeze–thawed		150 freeze–thaw Cycles	
	D_{MAX} (mm)	*p* (%)	D_{MAX} (mm)	*p* (%)
R25	4.218	0.0123	7.345	0.0151
R50	5.699	0.0132	7.825	0.0163
R75	3.627	0.014	4.402	0.017
RC25-NT1.2	4.260	0.0097	6.97	0.0129
RC50-NT1.2	3.590	0.0103	4.822	0.0138
RC75-NT1.2	7.398	0.0117	9.312	0.0151

D_{MAX} represents the maximum pore size, and *p* represents the porosity of the maximum pore.

3.3. Microstructure Analysis

Figure 10 is the SEM scanning electron micrograph of RC25-NT1.2 group recycled aggregate concrete before and after freeze–thaw damage. As can be seen from Figure 10a, when not freeze–thawed, the overall structure of recycled aggregate concrete is compact, the old and new mortar interface is separated by cracks, and partition is obvious. The surface of the new mortar is relatively flat, and the surface of the old mortar is honeycomb, with more deposits and a small number of fine cracks. After an enlarged observation, there are no obvious pores and cracks inside. There are a large number of spherical particles of C–S–H gel and a small amount of needle-like ettringites (AFt) around the aggregate, which are connected and stacked with each other, increasing the mechanical bite force between RCA and cement-based materials, forming a dense spatial network structure. After 150 freeze–thaw cycles, as shown in Figure 10b, the recycled aggregate concrete surface cement-mortar-shedding phenomenon is serious, with loose structure, visible clear coarse aggregate, and a large number of cracks interlaced throughout the surface. The internal pores increase, the distribution of C–S–H gel is uneven, and there are a small number of plate-like CH crystals. It can be seen that the coarse aggregate is not completely wrapped, the cement hydration in the adjacent space of the aggregate is not sufficient, and there are obvious cracks and interface transition zones.

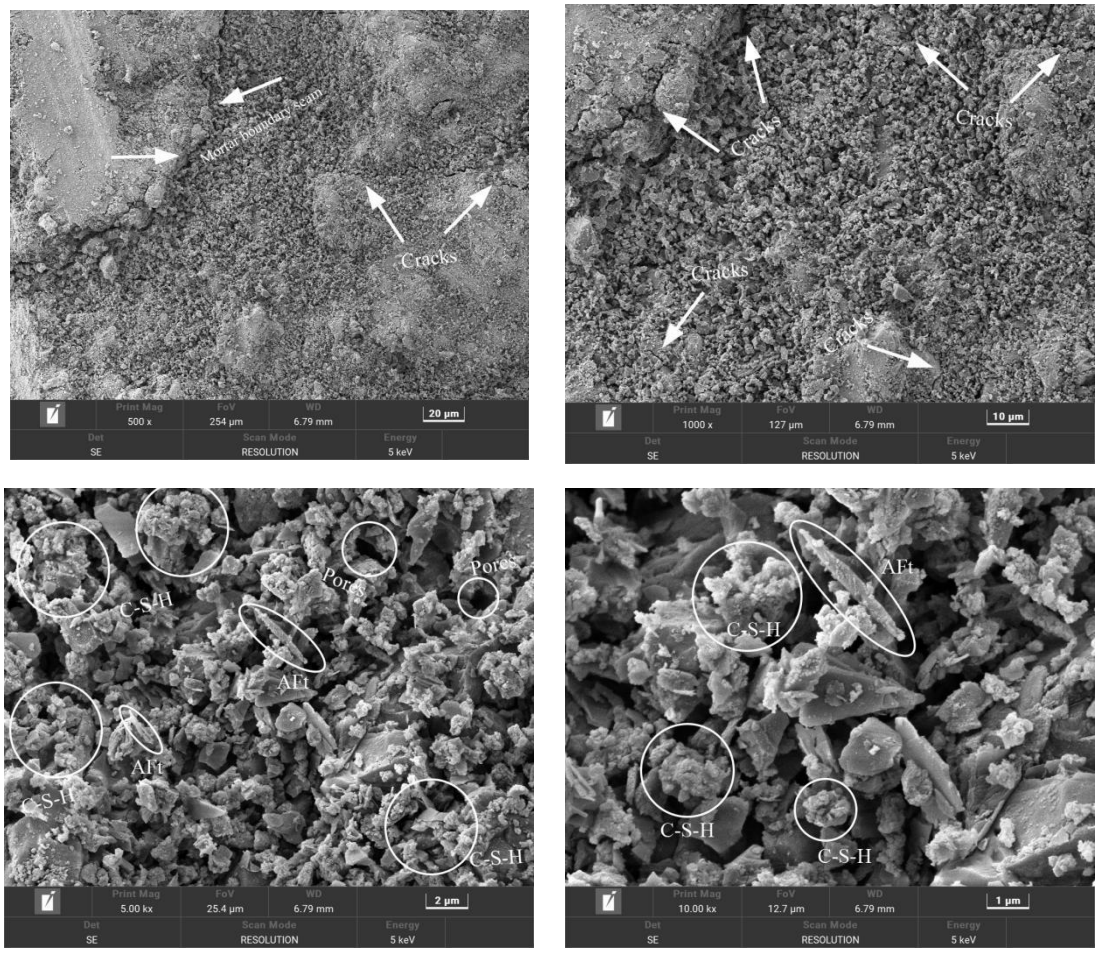

(**a**)

Figure 10. *Cont.*

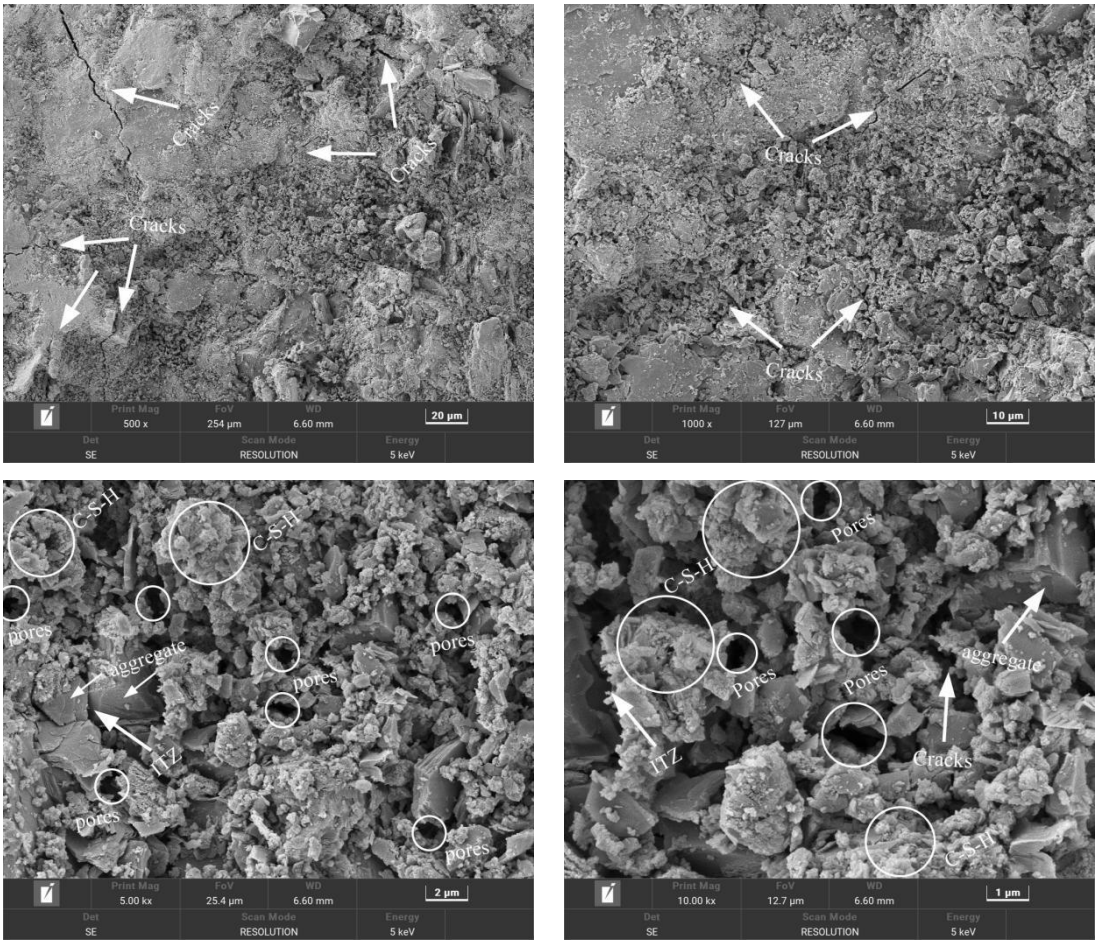

(**b**)

Figure 10. Microstructure of recycled aggregate concrete before and after freeze–thaw damage. (**a**) Freeze–thaw cycle 0 times; (**b**) Freeze–thaw cycle 150 times.

From the pore-distribution map, it can be seen that nano-TiO_2 can refine the pore structure. It can be seen from the SEM image that the hydration products generated by nano-TiO_2 hydration can fill the pores between the aggregate and the bulk slurry, enhance the interfacial adhesion between the aggregate and the cement stone, and form a dense microstructure [33,34]. Under the same freeze–thaw cycle conditions, the volume of water in the pores changes, the amount of icing decreases, the concrete structure is denser, and the ability to resist freeze–thaw cycle damage is enhanced. However, under uninterrupted freeze–thaw cycles, the cracks in RCA are prone to expansion, which will weaken the ameliorating effect of nano-TiO_2 and make the unfilled holes continue to split, affecting the stability of the internal structure of recycled concrete.

3.4. Prediction Model of Initial Capillary Water absorption

In the whole test process of nano-TiO_2 recycled aggregate concrete capillary water absorption, the size of the test block remains unchanged, and always remains in a one-dimensional water-absorption state to ensure that the water transport direction inside the recycled aggregate concrete is consistent. Before the test begins, the inside and outside of the test block are always in a completely dry state. During the water-absorption process, the water-absorption boundary conditions are stable. Nano-TiO_2 recycled aggregate concrete initial capillary water absorption S_1 is proportional to the number of freeze–thaw cycles n growth and is positive.

According to the variation curve of the initial capillary water absorption S_1 of nano-TiO_2 recycled aggregate concrete with the number of freeze–thaw cycles n, the water-absorption prediction model of nano-TiO_2 recycled aggregate concrete under freeze–thaw cycles is obtained. Through data fitting, the expressions of the initial water absorption and the number of freeze–thaw cycles of recycled aggregate concrete under different freeze–thaw conditions are obtained [35].

$$S = AB^n \tag{4}$$

where S_1 is the initial capillary water absorption of recycled aggregate concrete; A and B are the influence coefficients of nano-TiO_2; n is the number of freeze–thaw cycles; and R^2 is the fitted regression coefficient. Table 9 shows the detailed parameters.

Table 9. Fitting parameters.

Number	*A*	*B*	R^2
RC25	0.04297	1.00357	0.96
RC25-NT0.4	0.03646	1.0044	0.96
RC25-NT0.8	0.03314	1.00464	0.95
RC25-NT1.2	0.03100	1.00485	0.97
RC50	0.04498	1.00376	0.96
RC50-NT0.4	0.03927	1.00424	0.96
RC50-NT0.8	0.03672	1.00444	0.97
RC50-NT1.2	0.03349	1.00471	0.95
RC75	0.04630	1.00393	0.95
RC75-NT0.4	0.04339	1.00412	0.96
RC75-NT0.8	0.04233	1.0043	0.97
RC75-NT1.2	0.04021	1.00436	0.97

The regression fit plot is shown in Figure 11.

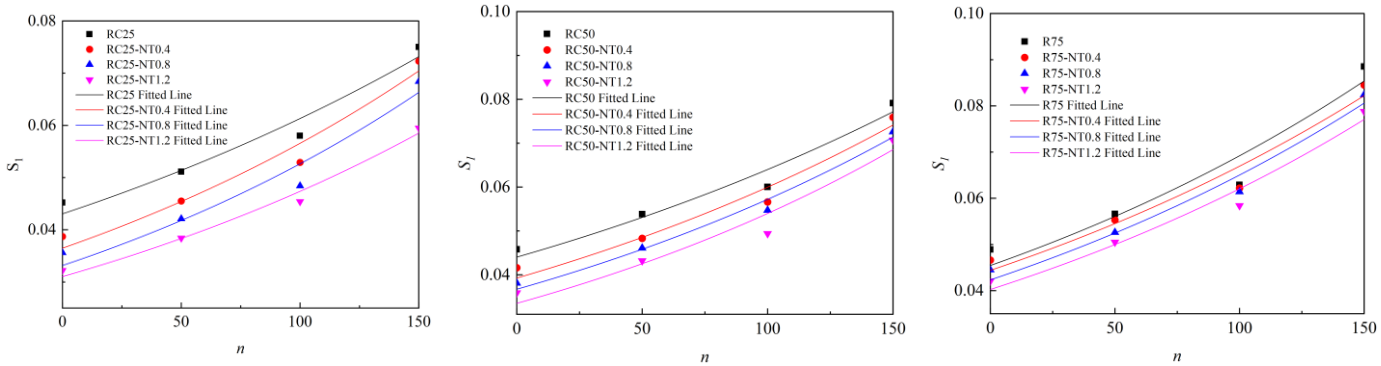

(**a**) (**b**) (**c**)

Figure 11. Fitted graph of water absorption S_1. (**a**) R25 group; (**b**) R50 group; (**c**) R75 group.

According to the regression analysis of the initial capillary water absorption of recycled aggregate concrete specimens with nano-TiO_2 contents of 0%, 0.4%, and 1.2% in each group, the relationship between the substitution rate of nano-TiO_2 and the influence coefficient of the substitution rate of nano-TiO_2 was established. Bringing A and B into Formula 4, the prediction model of the initial capillary water absorption of nano-TiO_2 recycled aggregate concrete under freeze–thaw cycles is shown in Table 10. The test block S_1 with the nano-TiO_2 content of 0.8% was brought into Table 10 for verification, and the relationship between the calculated value and the measured value of the prediction model was obtained, as shown in Figure 12. As shown in the regression plot, the data sample points are almost all distributed near the regression line, which indicates a good fit for the regression equation. Since the R^2 is around 0.96, it has been shown in the literature that R^2 above 0.90 indicates

an exact model and can be used for reference in the capillary-water-absorption test of nano-TiO_2 recycled aggregate concrete [36].

Table 10. Prediction model of initial capillary water absorption of Nano-TiO_2 recycled aggregate concrete.

Peer Group	Prediction Model of Initial Capillary Water Absorption
R25	$S = (0.0079{x_{NT}}^2 - 0.0194x_{NT} + 0.043) \times (-0.0019{x_{NT}}^2 + 0.0028x_{NT} + 1.0036)^n$
R50	$S = (0.0059{x_{NT}}^2 - 0.0166x_{NT} + 0.0450) \times (-0.0005x^2 + 0.0014x_{NT} + 1.0038)^n$
R75	$S = (0.0028{x_{NT}}^2 - 0.0084x_{NT} + 0.0463) \times (-0.0001x^2 + 0.0005x_{NT} + 1.0039)^n$

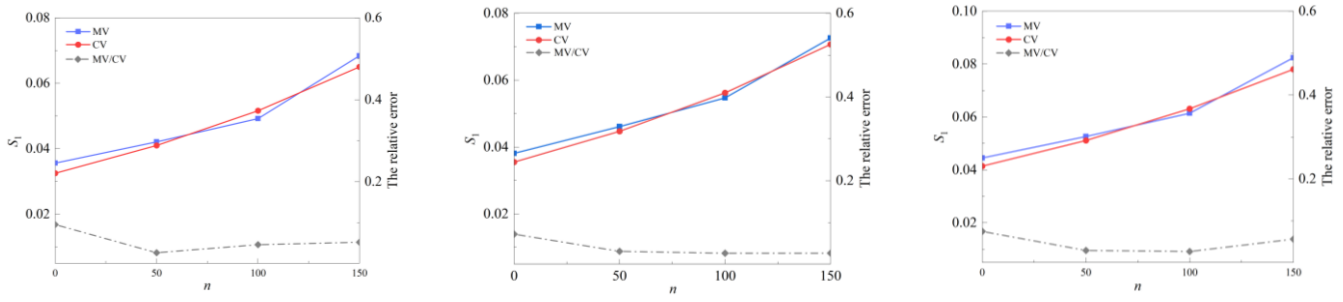

(**a**) (**b**) (**c**)

Figure 12. Relationship between measured and calculated values of the prediction model. (**a**) R25 group; (**b**) R50 group; (**c**) R75 group.

4. Conclusions

According to the experimental phenomena of 24 h capillary-water-absorption test and pore test before and after the freeze–thaw cycle of 12 groups of nano-TiO_2-recycled aggregate concrete with different dosages, the influence of nano-TiO_2 on recycled aggregate concrete is analysed from a macrolevel and a microlevel, respectively. According to the experimental phenomena and results, the following preliminary conclusions can be drawn:

(1) Adding nano-TiO_2 into recycled aggregate concrete can reduce the cumulative water absorption and porosity of recycled aggregate concrete and effectively improve the durability of concrete. Among them, 1.2% nano-TiO_2 content has the best repair effect on RCA surface pores and cracks.

(2) The variation curve of the cumulative water absorption shows that the initial capillary-water-absorption rate of nano-TiO_2 recycled concrete becomes a trend of present growth and then flat. The initial capillary-water-absorption rate, S_1, grows fast and large, and the secondary capillary-water-absorption rate, S_2, grows slowly and small. From the relationship curve of S_1 variation, the larger the nano-TiO_2 doping, the smaller the S_1; the larger the RCA substitution rate, the higher the S_1. The effect of S_2 on recycled concrete is negligible.

(3) The pore structure directly affects the capillary-water-absorption performance of recycled aggregate concrete, and the porosity is positively correlated with the capillary water absorption. Nano-TiO_2 can fill the gap between the aggregate, effectively alleviating the surface pores that evolved into cracks in the freeze–thaw cycle and enhancing the frost resistance of the recycled aggregate concrete. The porosity is positively correlated with the capillary-water-absorption rate of the recycled aggregate concrete. Moreover, according to SEM electron micrographs, it is seen that nano-TiO_2 can generate abundant hydration products after hydration, enhance the interfacial bonding force between aggregate and cement paste, and enhance the compactness of recycled aggregate concrete. However, a large number of freeze–thaw cycles will weaken the role of nano-TiO_2, resulting in sustained freeze–thaw damage.

(4) The established prediction model of initial capillary water absorption of nano-TiO_2recycled aggregate concrete under freeze–thaw cycles has been verified to be reliable.

(5) The authors believe that it is necessary to reproduce these experiments using different classes and different particle sizes of nanomaterials, which would make this study more rigorous.

Author Contributions: Conceptualization, C.Z., Z.Y., P.T. and Y.L.; methodology, C.Z., Z.Y., J.Z. and P.T.; software, Z.Y., Y.L. and P.T.; validation, C.Z., J.Z. and J.C.; writing—original draft preparation, C.Z., Z.Y. and P.T.; writing—review and editing, C.Z., Z.Y., J.Z., Y.L. and P.T.; visualization, C.Z., J.Z. and J.C.; project administration, C.Z., J.Z. and J.C.; funding acquisition, C.Z., J.Z. and J.C. All authors have read and agreed to the published version of the manuscript.

Funding: This research was funded by the National Natural Science Foundation of China (grant number 52208340), the State Key Laboratory of Bridge Structure Health and Safety (grant number BHSKL19–04–KF), the Project of Outstanding Young and Middle-aged Scientific and Technological Innovation Team in Hubei Universities and Colleges (grant number T2022010), and the Doctoral Start-up Fund of Hubei University of Technology (grant number BSQD2020051).

Institutional Review Board Statement: Not applicable.

Informed Consent Statement: Not applicable.

Data Availability Statement: The data used to support the findings of this study are available from the corresponding authors upon request.

Conflicts of Interest: The authors declare no conflict of interest.

References

1. Ho, H.J.; Iizuka, A.; Shibata, E. Chemical recycling and use of various types of concrete waste: A review. *J. Clean. Prod.* **2021**, *284*, 124785. [CrossRef]
2. Zhang, Y.; Luo, W.; Wang, J.; Wang, Y.; Xu, Y.; Xiao, J. A review of life cycle assessment of recycled aggregate concrete. *Constr. Build. Mater.* **2019**, *209*, 115–125. [CrossRef]
3. Makul, N.; Fediuk, R.; Amran, M.; Zeyad, A.M.; Murali, G.; Vatin, N.; Vasilev, Y. Use of recycled concrete aggregates in production of green cement-based concrete composites: A review. *Crystals* **2021**, *11*, 232. [CrossRef]
4. Al Ajmani, H.; Suleiman, F.; Abuzayed, I.; Tamimi, A. Evaluation of concrete strength made with recycled aggregate. *Buildings* **2019**, *9*, 56. [CrossRef]
5. McGinnis, M.J.; Davis, M.; de la Rosa, A.; Weldon, B.D.; Kurama, Y.C. Strength and stiffness of concrete with recycled concrete aggregates. *Constr. Build. Mater.* **2017**, *154*, 258–269. [CrossRef]
6. Wang, R.; Yu, N.; Li, Y. Methods for improving the microstructure of recycled concrete aggregate: A review. *Constr. Build. Mater.* **2020**, *242*, 118164. [CrossRef]
7. Zhang, P.; Wittmann, F.H.; Vogel, M.; Müller, H.S.; Zhao, T. Influence of freeze-thaw cycles on capillary absorption and chloride penetration into concrete. *Cement. Concrete. Res.* **2017**, *100*, 60–67. [CrossRef]
8. Lian, S.; Ruan, S.; Zhan, S.; Unluer, C.; Meng, T.; Qian, K. Unlocking the role of pores in chloride permeability of recycled concrete: A multiscale and a statistical investigation. *Cement. Concrete. Comp.* **2022**, *125*, 104320. [CrossRef]
9. Danish, A.; Mosaberpanah, M.A. A review on recycled concrete aggregates (RCA) characteristics to promote RCA utilization in developing sustainable recycled aggregate concrete (RAC). *Eur. J. Environ. Civ. Eng.* **2022**, *26*, 6505–6539. [CrossRef]
10. Eckert, M.; Oliveira, M. Mitigation of the negative effects of recycled aggregate water absorption in concrete technology. *Constr. Build. Mater.* **2017**, *133*, 416–424. [CrossRef]
11. Li, H.; Zhang, Y.; Guo, H. Numerical Simulation of the Effect of Freeze–Thaw Cycles on the Durability of Concrete in a Salt Frost Environment. *Coatings* **2021**, *11*, 1198. [CrossRef]
12. Júnior, N.A.; Silva, G.A.O.; Ribeiro, D.V. Effects of the incorporation of recycled aggregate in the durability of the concrete submitted to freeze-thaw cycles. *Constr. Build. Mater.* **2018**, *161*, 723–730. [CrossRef]
13. Junak, J.; Sicakova, A. Effect of surface modifications of recycled concrete aggregate on concrete properties. *Buildings* **2017**, *8*, 2. [CrossRef]
14. Kazmi, S.M.S.; Munir, M.J.; Wu, Y.F.; Patnaikuni, I.; Zhou, Y.; Xing, F. Influence of different treatment methods on the mechanical behavior of recycled aggregate concrete: A comparative study. *Cement. Concrete. Comp.* **2019**, *104*, 103398. [CrossRef]
15. El-Hawary, M.; Al-Yaqout, A.; Elsayed, K. Freezing and thawing cycles: Effect on recycled aggregate concrete including slag. *Int. J. Sustain. Eng.* **2021**, *14*, 800–808. [CrossRef]
16. Santana Rangel, C.; Amario, M.; Pepe, M.; Martinelli, E.; Toledo Filho, R.D. Durability of structural recycled aggregate concrete subjected to Freeze-Thaw cycles. *Sustainability* **2020**, *12*, 6475. [CrossRef]
17. Wang, J.J.; Xue, S.B.; Zhang, P.; Li, C.Y.; Gao, S.Z. Effect of Air Entraining Agent on Capillary Water Absorption of Mortar Before and After Freeze-Thaw Cycles. *J. Build. Mater.* **2022**, *25*, 1007–1014.

18. Deboucha, W.; Oudjit, M.N.; Bouzid, A.; Belagraa, L. Effect of incorporating blast furnace slag and natural pozzolana on compressive strength and capillary water absorption of concrete. *Procedia Eng.* **2015**, *108*, 254–261. [CrossRef]
19. Balapour, M.; Joshaghani, A.; Althoey, F. Nano-SiO_2 contribution to mechanical, durability, fresh and microstructural characteristics of concrete: A review. *Constr. Build. Mater.* **2018**, *181*, 27–41. [CrossRef]
20. Bautista-Gutierrez, K.P.; Herrera-May, A.L.; Santamaría-López, J.M.; Honorato-Moreno, A.; Zamora-Castro, S.A. Recent progress in nanomaterials for modern concrete infrastructure: Advantages and challenges. *Materials* **2019**, *12*, 3548. [CrossRef]
21. Bica, B.O.; de Melo, J.V.S. Concrete blocks nano-modified with zinc oxide (ZnO) for photocatalytic paving: Performance comparison with titanium dioxide (TiO_2). *Constr. Build. Mater.* **2020**, *252*, 119120. [CrossRef]
22. Li, G.; Cui, H.; Zhou, J.; Hu, W. Improvements of nano-TiO_2 on the long-term chloride resistance of concrete with polymer coatings. *Coatings* **2019**, *9*, 323. [CrossRef]
23. Liu, F.; Zhang, T.; Luo, T.; Zhou, M.; Ma, W.; Zhang, K. The effects of Nano-SiO_2 and Nano-TiO_2 addition on the durability and deterioration of concrete subject to freezing and thawing cycles. *Materials* **2019**, *12*, 3608. [CrossRef] [PubMed]
24. Ying, J.; Zhou, B.; Xiao, J. Pore structure and chloride diffusivity of recycled aggregate concrete with nano-SiO_2 and nano-TiO_2. *Constr. Build. Mater.* **2017**, *150*, 49–55. [CrossRef]
25. Chen, J.; Kou, S.C.; Poon, C.S. Hydration and properties of nano-TiO_2 blended cement composites. *Cement. Concrete. Comp.* **2012**, *34*, 642–649. [CrossRef]
26. *GB/T 50082-2009*; Standard for test methods of long-term performance and durability of ordinary concrete. General Administration of Quality Supervision, Inspection and Quarantine of the People's Republic of China (AQSIQ) and Ministry of Housing and Urban-Rural Development of the People's Republic of China (MOHURD): Beijing, China, 2009.
27. Djerbi, A. Effect of recycled coarse aggregate on the new interfacial transition zone concrete. *Constr. Build. Mater.* **2018**, *190*, 1023–1033. [CrossRef]
28. Memon, S.A.; Bekzhanova, Z.; Murzakarimova, A. A Review of Improvement of Interfacial Transition Zone and Adherent Mortar in Recycled Concrete Aggregate. *Buildings* **2022**, *12*, 1600. [CrossRef]
29. Ma, B.; Li, H.; Mei, J.; Li, X.; Chen, F. Effects of nano-TiO_2 on the toughness and durability of cement-based material. *Adv. Mate. Sci. Eng.* **2015**, *2015*, 583106.
30. Zhang, R.; Cheng, X.; Hou, P.; Ye, Z. Influences of nano-TiO_2 on the properties of cement-based materials: Hydration and drying shrinkage. *Constr. Build. Mater.* **2015**, *81*, 35–41. [CrossRef]
31. Akono, A.T. Effect of nano-TiO_2 on C–S–H phase distribution within Portland cement paste. *J. Mater. Sci.* **2020**, *55*, 11106–11119. [CrossRef]
32. Salman, M.M.; Eweed, K.M.; Hameed, A.M. Influence of partial replacement TiO_2 nanoparticles on the compressive and flexural strength of ordinary cement mortar. *Al-Nahrain J. Eng. Sci.* **2016**, *19*, 265–270.
33. Li, Z.; Han, B.; Yu, X.; Dong, S.; Zhang, L.; Dong, X.; Ou, J. Effect of nano-titanium dioxide on mechanical and electrical properties and microstructure of reactive powder concrete. *Mater. Res. Express* **2017**, *4*, 095008. [CrossRef]
34. Ren, Z.; Liu, Y.; Yuan, L.; Luan, C.; Wang, J.; Cheng, X.; Zhou, Z. Optimizing the content of nano-SiO_2, nano-TiO_2 and nano-$CaCO_3$ in Portland cement paste by response surface methodology. *J. Build. Eng.* **2021**, *35*, 102073. [CrossRef]
35. Xiao, Q.; Liu, X.; Qiu, J.; Li, Y. Capillary water absorption characteristics of recycled concrete in Freeze-Thaw environment. *Adv. Mater. Sci. Eng.* **2020**, *2020*, 1620914. [CrossRef]
36. Iqbal, M.F.; Liu, Q.F.; Azim, I.; Zhu, X.; Yang, J.; Javed, M.F.; Rauf, M. Prediction of mechanical properties of green concrete incorporating waste foundry sand based on gene expression programming. *J. Hazard. Mater.* **2020**, *384*, 121322. [CrossRef] [PubMed]